Simulation of a Chemical Vapor Deposition: Four phase model

J.GEISER[1], and M.ARAB[2]

[1]*Humboldt-Universität zu Berlin,Department of Mathematics, Unter den Linden 6, D-10099 Berlin, Germany*

Email: geiser@mathematik.hu-berlin.de

[2]*Humboldt-Universität zu Berlin, Department of Mathematics, Unter den Linden 6, D-10099 Berlin, Germany*

Email: arab@mathematik.hu-berlin.de

ABSTRACT

We are motivated to model chemical vapor deposition for metallic bipolar plates and optimization to deposit a homogeneous layer. Moreover a constraint to the deposition process is a very low pressure (nearly vacuum) and a low temperature (about 400 K). These constraints need to have a catalyst process, here in our apparatus we deal with a plasma source and precursor gases, see (Dobkin and Zuraw 2003). Such a plasma have the advantage to accelerate the vaporation process, see (Lieberman and Lichtenberg 2005), and to bring the solid materials to a gaseous phase. Nevertheless there are also some drawbacks, so that a retardation and adsorption process can hinder the direct transport to the target, see (Lieberman and Lichtenberg 2005).

Here, we present a mesoscopic model, which reflects the retardation, transport and reaction of the gaseous species through a homogeneous media in the chamber. The models include immobile gaseous phases, where the transport of the mobile gaseous species are hindered. Kinetically controlled adsorption are included to taken into account the multiple species of heavier and lighter species. Such ideas are also considered in fluid dynamical models, see (Farooq and Ruthven 1991). Further, the models include the conservation of mass and the porous media,

are in accordance with the Darcy‘s law, which is an assumption to the flow processes of the gaseous phase. The transport through the instationary and ionized plasma field is treated as a diffusion-dominated flow with mobile and immobile zones, see (Gobbert and Ringhofer 1998) and (Lieberman and Lichtenberg 2005), where the metallic deposit and the gas chamber, looking like a porous media, (Rouch 2006; Cao and Burggraaf 1993). We have a continuity condition and an overall balance, where we detailed model the temporal development of sorption processes. For the kinetics we apply first order processes and reflecting the different time-scales of the multi gaseous species. We choose porous ceramic membranes and gas catalysts like Argon (Ar), (Cao and Burggraaf 1993), additionally we assume precursor gases like Chlor (Cl) and apply our experience in simulating gaseous flow and modeling the penetration of such porous media, (Jin and Wang 2002).

Numerical methods are developed to solve such multi-scale and multi-phase models and to obtain qualitative results of the delicate multi physical processes in the gas chamber. To solve such evolution models, we combine discretization methods for partial differential and ordinary differential equations. Sequentially treatment of the partial differential equations and ordinary differential equations allow to discretize with Finite volume methods for the spatial derivatives of the transport equations, while Runge-Kutta methods are used to discretize the time derivatives and the ordinary parts of the multi-phase model. With various source terms we control the required concentration at the final deposition area. Different kinetically parameters allow to simulate the different time scale of the heavier and lighter gaseous species. We present an expert system based on a multi phase model and embedded source and target controls to present an accurate computational models for the transport of gas concentrations to a plasma media. For such efficient choose of models an discussion of physically correct numerical methods are important and simulate an optimal homogeneous deposition at the target with control of the rest gaseous concentration in the plasma media. The results are discussed by means of physical experiments to give a valid model for the assumed growth.

Keywords: Chemical vapor deposition, multi-scale problem, multi-phase problem, discretization methods, multi-species problem.

AMS subject classifications. 35K25, 35K20, 74S10, 70G65.

1 INTRODUCTION

We motivate our study by simulating a growth of a thin film that can be done by PE-CVD (plasma enhanced chemical vapor deposition) processes, see (Lieberman and Lichtenberg 2005) and (Ohring 2002). Further methods based on ionized plasma for deposition methods are PVD (physical vapor deposition) processes. If we only concentrate on the macroscopic transport of gaseous species, we can also lightly modify our models and simulate also PVD processes, taken into account clusters of heavier and lighter species, see (Senega and Brinkmann 2007). A gas exposed to an electric field in low pressure conditions $(< 5$ Torr$)$ results in a non-equilibrium plasma, see (Chapman 1980) and (Morosoff 1990), such ionized media, known as "cold" plasma or glow discharges, are powerful surface-modification tools in Material Science and Technology. Low-pressure plasmas allow to modify the surface chemistry and properties of materials compatible with low-medium vacuum, through a PE-CVD process, see applications (Favia and D'Agostino 2002) and (Morosoff 1990).

Due to control this PE-CVD process has been interested on producing high-temperature films, see (Ohring 2002).

While having a powerful deposition process in low-temperature and low-pressure regimes, we have also taken into account some drawbacks of such a process, which is driven with ionized plasma. Here, we deal with multicomponent problems with heavier and lighter species. Such conditions have consequences in slower (strongly adsorbed) or faster traveling (waker adsorbed) species.

To model the gaseous transport of our deposition process, in an ionized plasma, we present a multi-phase and multi-species model and deal with the underlying plasma as a media with mobile and immobile phases or groups, see (Favia and D'Agostino 2002) and (Lieberman and Lichtenberg 2005). The species of the gaseous transport are MAX-phase materials, see (Barsoum and El-Raghy 1996), (Du and Aldinger 2000) and (Lange and Schaaf 2007), and we concentrate on Ti_3SiC_2 molecules, so we have Ti, Si and C in the gas phases.

For the underlying multiple phase motivation, we apply a four phase model, that was developed for fluid dynamical problems, see (Fein 2004) and (Farooq and Ruthven 1991). We have taken into account the extension to a gaseous transport model, while dealing with a low-temperature and low-pressure environment in an ionized plasma, see (Senega and Brinkmann 2007). For the mobile phase we consider a transport models that are related to mesoscopic scales, (Gobbert and Ringhofer 1998), with respect to flows close to the wafer surface. Such a wafer surface can be modeled as a porous media, (Rouch 2006).

By assuming a ionized plasma that activate the particle transport to the deposition layer, PE-CVD process can be assumed as a homogeneous media, while dealing with ionized media and/or gas catalysts (Argon, Xenon). Such media itself has mobile and immobile phases in which the gaseous particles are transported or retarded, see (Serdyuk and Gubanski 2005). Further we taken into account the different precursor gases (e.g. Silane SiH_4), which have additionally sorbed processes to the deposition gases (Ti, Si, C), see an experimental application (Lemieux and Zhang 2008).

We assume to model the ionized plasma as an underlying media in the chamber with mobile and immobile phases. Here transport in the plasma with gaseous species contain of mobile and immobile concentrations, (Lieberman and Lichtenberg 2005). For such a homogenous plasma, we applied our expertise in modeling multiphase transport through a porous medium.

To amplify the modeling of the gaseous flow to the gas chamber which is filled with ionized plasma, we deal with the so-called far-field model based on a porous media. Here the plasma can be modeled as a continuous flow (Gobbert and Ringhofer 1998), that has mobile and immobile phases, see (Favia and D'Agostino 2002).

We assume a near vacuum and a diffusion-dominated process, derived from the Knudsen diffusion, (Cao and Burggraaf 1993). In such viscous flow regimes, we deal with small Knudsen Numbers and a pressure of nearly zero.

In Figure 1, the gas chamber of the CVD apparatus is shown, which is done with a porous media.

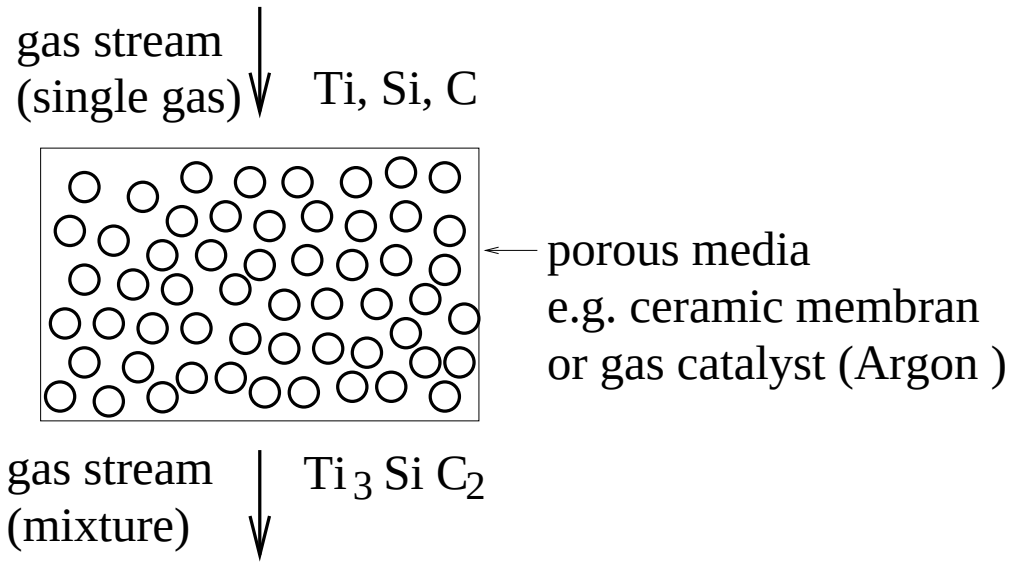

Figure 1: Gas chamber of the CVD apparatus.

In Figure 2, the mobile and immobile phases of the gas concentration are shown in the macroscopic scale of the porous media.

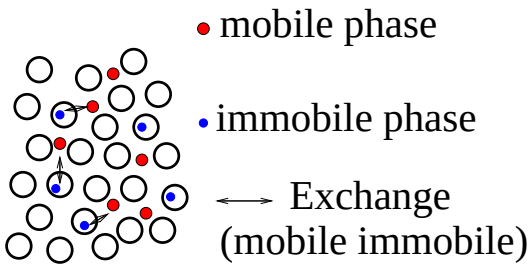

Figure 2: Mobile and immobile phase.

In Figure 3, the mobile and adsorbed phases of the gas concentration are shown in the macroscopic scale of the porous media.

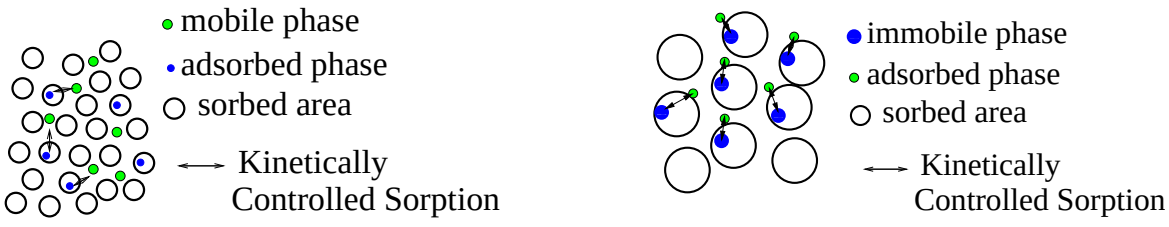

Figure 3: Mobile-adsorbed phase and immobile-adsorbed phase.

To solve the model, we concentrate on numerical solvers and discretization methods, that taken into account the individual time- and spatial scales of each equation part. To decompose the time and spatial scales with the different discretization methods are to obtain efficiency in the solver processes.

The immobile, adsorbed and reaction terms can be treated with fast Runge-Kutta solvers, where the mobile terms are convection-diffusion equations and are solved with splitting semi-implicit finite volume methods and characteristic methods, (Geiser 2006).

The numerical results discuss the applications in the production of so-called metallic bipolar plates. Here we discuss analytical and numerical models.

The paper is outlined as follows.

In Section 2, we present our mathematical model and a possible reduced model for further approximations. In Section 3, we discuss the time- and space-discretization methods with respect to the efficiency and accuracy. The numerical experiments are given in Section 4. In Section 5, we briefly summarize our results.

2 MATHEMATICAL MODEL

In the following, the models are discussed in terms of transport problem on a macro- or mesoscopic scale, multiphase model with sorbed and immobile zones:

1. Transport model (Gobbert and Ringhofer 1998) (mesoscopic scale);
2. Multiphase model (Lemieux and Zhang 2008), (Fein 2004) (kinetic sorption, mobile-immoble zones).
3. Multicomponent model (Senega and Brinkmann 2007) (lighter-heavier species).

The modeling is considered by a Knudsen Number, which is the ratio of the mean free path λ over the typical domain size L. For small Knudsen Numbers $Kn \approx 0.01 - 1.0$ we deal with

mass conservation, whereas for large Knudsen Numbers $Kn \geq 1.0$ we deal with a Boltzmann equation (Ohring 2002).

We concentrate on a mesoscopic model and assume a continuum flow, and that the fluid equations can be treated with a Navier-Stokes or especially with a convection-diffusion-reaction equation, see:

$$\frac{\partial}{\partial t}c + \nabla F - R_g = 0, \text{ in } \Omega \times [0,t] \tag{1}$$
$$F = \mathbf{v}c - D\nabla c,$$
$$c(x,t) = c_0(x), \text{ on } \Omega, \tag{2}$$
$$c(x,t) = c_1(x,t), \text{ on } \partial\Omega \times [0,t], \tag{3}$$

where c is the molar concentration and F the flux of the species. $\mathbf{v}$ is the flux velocity through the chamber and porous substrate (Rouch 2006). D is the diffusion matrix and R_g is the reaction term. The initial value is given as c_0 and we assume a Dirichlet boundary with the function $c_1(x,t)$ sufficiently smooth.

The diffusion in the modified CVD process is given by the Knudsen diffusion, (Cao and Burggraaf 1993). We consider the overall pressure in the reactor is $200\ Pa$ and the substrate temperature is about $600 - 900\ K$. The pore size in the porous substrate is $80\ nm$.

The diffusion is described as:

$$D = \frac{2\epsilon\mu_K\nu r}{3RT}, \tag{4}$$

where ϵ is the porosity, μ_K is the shape factor of the Knudsen diffusion, r is the average pore radius, R and T are the gas constant and temperature, respectively, and ν is the mean molecular speed, given by:

$$\nu = \sqrt{\frac{8RT}{\pi W}}, \tag{5}$$

where W is the molar mass of the diffusive gas.

For the homogeneous reactions, we consider during the CVD process a constant reaction of Si, Ti and C given as:

$$3Si + Ti + 2C \rightarrow Si_3TiC_2, \tag{6}$$

where Si_3TiC_2 is a MAX-phase material, which deposits at the target.

For simplification, we do not consider the intermediate reaction with the precursor gases, (Lieberman and Lichtenberg 2005).

The reaction rate is then given by:

$$\lambda = k_r \frac{[3Si]^M [Ti]^N [2C]^O}{[Si_3TiC_2]^L}, \tag{7}$$

where k_r is the apparent reaction constant, L, M, N, O are the reaction orders of the reactants.

The velocity in the homogeneous substrate is modeled by a porous medium (Bear 1972; Johannsen 1999). We have assumed a stationary medium, e.g. non-ionized plasma or non-reactive precursor gas. Further the pressure can be assumed with the Maxwell distribution as (Lieberman and Lichtenberg 2005) :

$$p = \rho bT, \tag{8}$$

where b is the Boltzmann's constant and T the temperature.

We have modeled the velocity by partial differential equations. Here we assume the gaseous flow is a nearly liquid flow through the porous medium. We can therefore derive by Darcy's

law:

$$\boldsymbol{v} = -\frac{k}{\mu}(\nabla p - \rho g)\,, \tag{9}$$

where $\boldsymbol{v}$ is the velocity of the fluid, k is the permeability tensor, μ is the dynamic viscosity, p is the pressure, g is the vector of the gravity and ρ is the density of the fluid.

We use the continuum equation of the particle density and obtain the equation of the system, which is given as our flow equation:

$$\partial_t(\phi\rho) + \nabla \cdot (\rho \boldsymbol{v}) = Q\,, \tag{10}$$

where ρ is the unknown particle density, ϕ is the effective porosity and Q is the source-term of the fluid. We assume a stationary fluid and consider only divergence-free velocity fields, i.e.

$$\nabla \cdot \boldsymbol{v}(x) = 0\,, \quad x \in \Omega\,. \tag{11}$$

The boundary conditions for the flow equation are given as:

$$p = p_r(t,\gamma), \quad t > 0\,, \quad \gamma \in \partial\Omega\,, \tag{12}$$

$$\boldsymbol{n} \cdot \boldsymbol{v} = m_f(t,\gamma), \quad t > 0\,, \quad \gamma \in \partial\Omega\,, \tag{13}$$

where $\boldsymbol{n}$ is the normal unit vector with respect to $\partial\Omega$, where we assume that the pressure p_r and flow concentration m_f are prescribed by Dirichlet boundary conditions (Johannsen 1999).

From the stationary fluid, we assume that the conservation of momentum for velocity $\boldsymbol{v}$ is given (Glowinski 2003; Johannsen 1999). So we can neglect the computation of the momentum for the velocity.

For the kinetically controlled sorption, we apply the Henry isotherms as a simple incorporated temporal development of our sorption processes.

The mass transfer rates of the kinetic sorptions are given as:

$$\phi \partial_t c_{i,ad}^L = k_\alpha (c_i^L - c_{i,ad}^L), \tag{14}$$

where k_α is the exchange rate. $c_{i,ad}^L$ is the adsorbed concentration to the mobile concentration c_i^L.

Remark 1 *For the flow through the gas chamber, for which we assume a homogeneous medium and non-reactive plasma, we have considered a constant flow (Hlavacek and Orlicki 1995). A further simplification is given by the very small porous substrate, for which we can assume the underlying velocity in a first approximation as constant (Ohring 2002).*

Remark 2 *For an instationary medium and reactive or ionized plasma, we have to be taken into account the relations of the electrons in the thermal equilibrium. Such spatially variation can be considered by modeling the electron drift. Such modeling of the ionized plasma is done with the Boltzmanns relation, (Lieberman and Lichtenberg 2005).*

2.1 Transport model of mobile immobile and adsorbed zones

In the following we present the multiphase transport model.

$$\begin{aligned} &\phi \partial_t c_i^L + \nabla \cdot (\mathbf{v} c_i^L - D^{e(i)} \nabla c_i^L) = g(-c_i^L + c_{i,im}^L) + k_\alpha (-c_i^L + c_{i,ad}^L \\ &-\lambda_{i,i} \phi c_i^L + \sum_{k=k(i)} \lambda_{i,k} \phi c_k^L + \tilde{Q}_i, \end{aligned} \tag{15}$$

$$\phi \partial_t c_{i,im}^L = g(c_i^L - c_{i,im}^L) + k_\alpha (c_{i,im,ad}^L - c_{i,im}^L) - \lambda_{i,i} \phi c_{i,im}^L + \sum_{k=k(i)} \lambda_{i,k} \phi c_{k,im}^L + \tilde{Q_{i,im}}, \tag{16}$$

$$\phi \partial_t c^L_{i,ad} = k_\alpha (c^L_i - c^L_{i,ad}) - \lambda_{i,i} \phi c^L_{i,ad} + \sum_{k=k(i)} \lambda_{i,k} \phi c^L_{k,ad} + \tilde{Q_{i,ad}}, \tag{17}$$

$$\phi \partial_t c^L_{i,im,ad} = k_\alpha (c^L_{i,im} - c^L_{i,im,ad}) - \lambda_{i,i} \phi c^L_{i,im,ad} + \sum_{k=k(i)} \lambda_{i,k} \phi c^L_{k,im,ad} + \tilde{Q_{i,im,ad}}, \tag{18}$$

ϕ : effective porosity $[-]$,

c^L_i : concentration of the ith gaseous species in the plasma chamber

$c^L_{i,im}$: concentration of the ith gaseous species in the immobile zones of the plasma chamber phase $[mol/cm^3]$,

$\mathbf{v}$: velocity in the plasma chamber $[cm/nsec]]$,

$D^{e(i)}$: element-specific diffusions-dispersions tensor $[cm^2/nsec]]$,

$\lambda_{i,i}$: decay constant of the ith species $[1/nsec]]$,

$\tilde{Q}_i$: source term of the ith species $[mol/(cm^3 nsec)]$,

g : exchange rate between the mobile and immobile concentration $[1/nsec]$,

k_α : exchange rate between the mobile and adsorbed concentration or immobile and immobile adsorbed concentration (kinitic controlled sorption) $[1/nsec]$,

with $i = 1, \ldots, M$ and M denotes the number of components.

The parameters in equation (15) are further described, see also (Geiser 2003).
The effective porosity is denoted by ϕ and declares the portion of the porosities of the aquifer, that is filled with plasma, and we assume a nearly fluid phase. The transport term is indicated by the Darcy velocity $\mathbf{v}$, that presents the flow-direction and the absolute value of the plasma flux. The velocity field is divergence-free. The decay constant of the ith species is denoted by λ_i. Thereby does $k(i)$ denote the indices of the other species.

In the following we describe the time- and space-discretization methods.

3 DISCRETIZATION AND SOLVER METHODS

We distinguish between mobile and immobile phases. Here the mobile phase are parabolic partial differential equations and the immobile phases are ordinary differential equations. So for the space-discretization of the PDE's we apply finite-volume methods as mass conserved discretization schemes and for the time-discretization of the PDE's and ODE's we apply Runge-Kutta methods. To accelerate the solver process, we combine numerical and analytical parts of the solutions.

In the next sections we introduce the notation for the space-discretization and describe the discretization-methods for each equation-part.

3.1 Discretization method of the convection equation

We deal with the following convection equation

$$\partial_t R\, c - \mathbf{v} \cdot \nabla c = 0 \;, \tag{19}$$

with the simple boundary condition $c = 0$ for the inflow and outflow boundary and the initial values $c(x_j, 0) = c_j^0(x)$. We use piecewise constant discretization method with the upwind discretization done in (Frolkovič and Geiser 2003) and get

$$\begin{aligned} V_j\, R\, c_j^{n+1} &= V_j\, R\, c_j^n - \tau^n \sum_{k \in out(j)} v_{jk}\, c_j^n + \tau^n \sum_{k \in in(j)} c_k^n\, v_{kj} \;, \\ V_j\, R\, c_j^{n+1} &= c_j^n (R\, V_j - \tau^n \nu_j) + \tau^n \sum_{k \in in(j)} c_k^n\, v_{kj} \;, \end{aligned} \tag{20}$$

The explicit time discretization has to fulfill the discrete minimum-maximum property (Frolkovič and Geiser 2003), and we get the following restriction for the time steps

$$\tau_j = \frac{R\, V_j}{\nu_j} \;, \quad \tau^n \leq \min_{j=1,\ldots,I} \tau_j \;. \tag{21}$$

To obtain improved spatial discretization methods and apply larger time-steps, we introduce a reconstruction with linear polynoms as a higher test-function in the next subsection.

3.2 Higher oder discretization method for the convection equation

The reconstruction is based on the Godunovs method and apply a limiter function that fulfilled the local min-max property. The method is explained in the paper (Frolkovič and Geiser 2003) and we discuss the algorithm in the following section.

The linear polynomes are reconstructed by the element-wise gradient and are given as

$$u^n(x_j) = c_j^n \ , \tag{22}$$

$$\nabla u^n|_{V_j} = \frac{1}{V_j} \sum_{e=1}^{E} \int_{T^e \cap \Omega_j} \nabla c^n dx \ , \tag{23}$$

$$\text{with} \quad j = 1, \ldots, I \ .$$

The piecewise linear functions are denoted as

$$u_{jk}^n = c_j^n + \psi_j \nabla u^n|_{V_j} (x_{jk} - x_j) \ , \tag{24}$$

$$\text{with} \quad j = 1, \ldots, I \ ,$$

where $\psi_j \in (0, 1)$ is the limiter function and based on this, the equation (27) fulfills the discrete minimum maximum property, as described in (Frolkovič and Geiser 2003).

We also use the limitation of the flux to get non overshooting, when transporting the mass and receive the maximal time-step.

We get the correct restriction due to the flux limiter and obtain the following concentration as

$$\tilde{u}_{jk}^n = u_{jk}^n + \frac{\tau_j}{\tau^n} (c_j^n - u_{jk}^n) \ . \tag{25}$$

Using all the previous schemes the discretization for the second order is written in the discretized form

$$RV_j c_j^{n+1} = RV_j c_j^n - \tau^n \sum_{k \in out(j)} \tilde{u}_{jk}^n v_{jk} + \tau^n \sum_{l \in in(j)} \tilde{u}_{lj}^n v_{lj} \ . \tag{26}$$

Based on this discretization method we can embed the reaction equation as a local effect, described in the following subsection.

3.3 Discretization method for the convection-reaction equation based on embedded one dimensional analytical solutions

We apply Godunovs method for the discretization method, cf. (Leveque 2002), and extend the formulation with analytical solution of convection-reaction equations. We reduce the multi-dimensional equation to one dimensional equations and solve each equation exactly. The one-dimensional solution is multiplied with the underlying volume and we get the mass-formulation. The one-dimensional mass is embedded into the multi-dimensional mass-formulation and we obtain the discretization of the multi-dimensional equation.

The algorithm is given in the following manner

$$\partial_t \ c_l + \nabla \cdot \mathbf{v}_l \ c_l = -\lambda_l \ c_l + \lambda_{l-1} \ c_{l-1},$$

with $l = 1, \ldots, m$.

The velocity vector $\mathbf{v}$ is divided by R_l. The initial conditions are given by $c_1^0 = c_1(x, 0)$, else $c_l^0 = 0$ for $l = 2, \ldots, m$ and the boundary conditions are trivial $c_l = 0$ for $l = 1, \ldots, m$.

We first calculate the maximal time step for cell j and concentration i with the use of the total outflow fluxes

$$\tau_{i,j} = \frac{V_j \ R_i}{\nu_j} \ , \quad \nu_j = \sum_{k \in out(j)} v_{jk} \ .$$

We get the restricted time step with the local time steps of cells and their components

$$\tau^n \leq \min_{\substack{i=1,\ldots,m \\ j=1,\ldots,I}} \tau_{i,j} \ .$$

The velocity of the discrete equation is given by

$$v_{i,j} = \frac{1}{\tau_{i,j}} \ .$$

We calculate the analytical solution of the mass, cf. (Geiser 2003) and we get

$$\begin{aligned} m^n_{i,jk,out} &= m_{i,out}(a, b, \tau^n, v_{1,j}, \ldots, v_{i,j}, R_1, \ldots, R_i, \lambda_1, \ldots, \lambda_i) \ , \\ m^n_{i,j,rest} &= m^n_{i,j} \ f(\tau^n, v_{1,j}, \ldots, v_{i,j}, R_1, \ldots, R_i, \lambda_1, \ldots, \lambda_i) \ , \end{aligned}$$

where $a = V_j R_i (c^n_{i,jk} - c^n_{i,jk'})$, $b = V_j R_i c^n_{i,jk'}$ and $m^n_{i,j} = V_j R_i c^n_{i,j}$. Further $c^n_{i,jk'}$ is the concentration at the inflow- and $c^n_{i,jk}$ is the concentration at the outflow-boundary of the cell j.

The discretization with the embedded analytical mass is calculated by

$$m^{n+1}_{i,j} - m^n_{i,rest} = - \sum_{k \in out(j)} \frac{v_{jk}}{\nu_j} \ m_{i,jk,out} + \sum_{l \in in(j)} \frac{v_{lj}}{\nu_l} \ m_{i,lj,out} \ ,$$

where $\frac{v_{jk}}{\nu_j}$ is the re-transformation for the total mass $m_{i,jk,out}$ in the partial mass $m_{i,jk}$. In the next time-step the mass is given as $m^{n+1}_{i,j} = V_j \ c^{n+1}_{i,j}$ and in the old time-step it is the rest mass for the concentration i. The proof is done in (Geiser 2003). In the next section we derive an analytical solution for the benchmark problem, cf. (Higashi and Pigford 1980), (Jury and Roth 1990).

In the next subsection we introduce the discretization of the diffusion-dispersion-equation.

3.4 Discretization of the diffusion-dispersion-equation

We discretize the diffusion-dispersion-equation with implicit time-discretization and finite-volume method for the following equation

$$\partial_t R\, c - \nabla \cdot (D \nabla c) = 0 \;, \tag{27}$$

where $c = c(x,t)$ with $x \in \Omega$ and $t \geq 0$. The diffusions-dispersions-tensor $D = D(x, \mathbf{v})$ is given by the Scheidegger-approach, cf. (Scheidegger 1961). The velocity is given as $\mathbf{v}$. The retardation-factor is $R > 0.0$.

The boundary-values are denoted by $\mathbf{n} \cdot D\ \nabla c(x,t) = 0$, where $x \in \Gamma$ is the boundary $\Gamma = \partial\Omega$, cf. (Frolkovič 2002a). The initial conditions are given by $c(x,0) = c_0(x)$.

We integrate the equation (27) over space and time and derive

$$\int_{\Omega_j} \int_{t^n}^{t^{n+1}} \partial_t R(c)\ dt\ dx = \int_{\Omega_j} \int_{t^n}^{t^{n+1}} \nabla \cdot (D \nabla c)\ dt\ dx \;. \tag{28}$$

The time-integration is done by the backward-Euler method and the diffusion-dispersion term is lumped, cf. (Geiser 2003)

$$\int_{\Omega_j} (R(c^{n+1}) - R(c^n))\ dx = \tau^n \int_{\Omega_j} \nabla \cdot (D \nabla c^{n+1})\ dx \;, \tag{29}$$

The equation (29) is discretized over the space with respect of using the Greens-formula.

$$\int_{\Omega_j} (R(c^{n+1}) - R(c^n))\ dx = \tau^n \int_{\Gamma_j} D\ \mathbf{n} \cdot \nabla c^{n+1}\ d\gamma \;, \tag{30}$$

where Γ_j is the boundary of the finite-volume cell Ω_j. We use the approximation in space, confer (Geiser 2003).

The spatial-integration for (30) is done by the mid-point rule over the finite boundaries and given as

$$V_j R(c_j^{n+1}) - V_j R(c_j^n) = \tau^n \sum_{e \in \Lambda_j} \sum_{k \in \Lambda_j^e} |\Gamma_{jk}^e| \mathbf{n}_{jk}^e \cdot D_{jk}^e \nabla c_{jk}^{e,n+1} \ , \tag{31}$$

where $|\Gamma_{jk}^e|$ is the length of the boundary-element Γ_{jk}^e. The gradients are calculated with the piecewise finite-element-function ϕ_l, cf. (**??**) and we obtain

$$\nabla c_{jk}^{e,n+1} = \sum_{l \in \Lambda^e} c_l^{n+1} \nabla \phi_l(\mathbf{x}_{jk}^e) \ . \tag{32}$$

We get with the difference-notation for the neighbor-point j and l, cf. (Frolkovič and De Schepper 2001) and get the discretised equation

$$\begin{aligned} &V_j R(c_j^{n+1}) - V_j R(c_j^n) = \\ &= \tau^n \sum_{e \in \Lambda_j} \sum_{l \in \Lambda^e \setminus \{j\}} \Big(\sum_{k \in \Lambda_j^e} |\Gamma_{jk}^e| \mathbf{n}_{jk}^e \cdot D_{jk}^e \nabla \phi_l(\mathbf{x}_{jk}^e) \Big) (c_j^{n+1} - c_l^{n+1}) \ , \end{aligned} \tag{33}$$

where $j = 1, \ldots, m$.

3.5 Discretization of the mobile, immobile and adsorbed parts

The full equation is given with a PDE and ODE part, see also equation (15), (16), (17) and (18).

We present in the following the discretisation of the mobile and immobile equations, the same can be done for the adsorbed equations.

$$\partial_t c_i = A c_i - g(c_i - c_{i,im}) \ , \tag{34}$$

$$\partial_t c_{i,im} = g(c_i - c_{i,im}) \ , \tag{35}$$

where c_i is the concentration in the mobile phase, $c_{i,im}$ is the concentration in the immobile phase, with $i = 1, \ldots, m$. Further g is the exchange rate between the mobile and immobile concentration. A is the matrix given by the spatial discretized operators of the equation (15).

The equation system is numerically solved by an iterative scheme:

Our algorithm is given as:

Algorithm 1 *We divide our time interval* $[0, T]$ *into sub-intervals* $[t^n, t^{n+1}]$*, where* $n = 0, 1, \ldots N$*,* $t^0 = 0$ *and* $t^N = T$*.*

We start with $n = 0$*:*

1.) The initial conditions are given with $c_i, 0(t^{n+1}) = c_i(t^n)$ *and* $c_{i,im,0}(t^{n+1}) = c_{i,im}(t^n)$*. We start with* $k = 0$*.*

2.) Compute the fix point iteration scheme given as:

$$\partial_t c_i^k = A c_i^k - g(c_i^k - c_{i,im}^{k-1}) \,, \tag{36}$$

$$\partial_t c_{i,im}^k = g(c_i^{k-1} - c_{i,im}^k) \,, \tag{37}$$

where k *is the iteration index, see (Farago I 2005). We apply Runge-Kutta methods as ODE solvers or simple implicit Euler methods.*

3.) The stop criterion for the time interval t^n, t^{n+1} *is given as:*

$$||c_i^k(t^{n+1}) - c_i^{k-1}(t^{n+1})|| \leq err, \tag{38}$$

$$||c_{i,im}^k(t^{n+1}) - c_{i,im}^{k-1}(t^{n+1})|| \leq err, \tag{39}$$

where $||\cdot||$ *is the maximum norm over all components of the solution vector.* err *is a given error bound, e.g.* $err = 10^{-4}$*.*

If equation (38) is fulfilled, we have the result

$$c_i(t^{n+1}) = c_{i,k}(t^{n+1}), \tag{40}$$

$$c_{i,im}(t^{n+1}) = c_{i,im}(t^{n+1}) \tag{41}$$

If $n = N$ then we stop and are done.

If not, we do $n = n + 1$, $k = 0$ and apply the initial conditions $c_i, 0(t^{n+1}) = c_i(t^n)$ and $c_{i,im,0}(t^{n+1}) = c_{i,im}(t^n)$.

If equation (38) is not fulfilled, we do $k = k + 1$ and goto 2.).

Numerical Methods to ODEs

For the ODE solvers we apply the following methods.

We use the implicit trapezoidal rule

$$\begin{array}{c|cc} 0 & & \\ 1 & \frac{1}{2} & \frac{1}{2} \\ \hline & \frac{1}{2} & \frac{1}{2} \end{array} \tag{42}$$

Further we use the following implicit Runge-Kutta methods:

Lobatto IIIA

$$\begin{array}{c|ccc} 0 & 0 & 0 & 0 \\ \frac{1}{2} & \frac{5}{24} & \frac{1}{3} & -\frac{1}{24} \\ 1 & \frac{1}{6} & \frac{2}{3} & -\frac{1}{6} \\ \hline & \frac{1}{6} & \frac{2}{3} & -\frac{1}{6} \end{array} \tag{43}$$

Remark 3 *We can also apply integration methods for the right hand side.*

3.6 Discretization of the source-terms

The source terms are part of the convection-diffusion equations and are given as follows:

$$\partial_t c_i(x,t) - \mathbf{v} \cdot \nabla c_i + \nabla D \nabla c_i = q_i(x,t) \ , \tag{44}$$

where $i = 1, \ldots, m$, $\mathbf{v}$ is the velocity, D is the diffusion tensor and $q_i(x,t)$ are the source functions, which can be pointwise, linear in the domain.

The pointwise sources are given as :

$$q_i(t) = \begin{cases} \frac{q_{s,i}}{T} & t \leq T, \\ 0 & t > T, \end{cases} \text{, with} \int_T q_i(t) dt = q_{s,i}, \tag{45}$$

where $q_{s,i}$ is the concentration of species i at source point $x_{source,i} \in \Omega$ over the whole time-interval.

The line and area sources are given as :

$$q_i(x,t) = \begin{cases} \frac{q_{s,i}}{T|\Omega_{source,i}|}, & t \leq T \text{ and } x \in \Omega_{source,i}, \\ 0, & t > T, \end{cases} \ , \tag{46}$$
$$\text{with} \int_{\Omega_{source,i}} \int_T q_i(x,t) dt dx = q_{s,i},$$

where $q_{s,i}$ is the source concentration of species i at the line or area of the source over the whole time-interval.

For the Finite volume discretization we have to compute :

$$\int_{\Omega_{source,i,j}} q_i(x,t) \ dx = \int_{\Gamma_{source,i,j}} \mathbf{n} \cdot (\mathbf{v} c_i - D \nabla c_i) \ d\gamma \ , \tag{47}$$

where $\Gamma_{source,i,j}$ is the boundary of the finite-volume cell $\Omega_{source,i,j}$ which is a source area. We have $\cup_j \Omega_{source,i,j} = \Omega_{source,i}$ where $j \in I_{source}$, where I_{source} is the set of the finite-volume cells that includes the area of the source.

The right hand side of (47) of is also called the flux of the sources, see (Frolkovič 2002b).

3.7 Solver method for the sources

The following algorithm is based on the iteration with additionally sequential splitting methods, see (Farago I 2005), that can be done parallel, while using multiple sources, see (Tai 1992).

On the time interval $[t^n, t^{n+1}]$ we solve the following problems :

$$\frac{\partial C(t)}{\partial t} = AC(t) \; + \; BC(t) \; + \sum_{j=1}^{m} Q_j(t) \text{ , with } \; C(t^n) = C^n \tag{48}$$

where $q_1, \ldots, q_m$ are the multiple sources and $C = (c, c_{im})^t$ consist of the mobile and immobile concentrations. $Q_j = (q_j, q_{j,im})^t$ is a source term of mobile and immobile source concentrations with $j = 1, \ldots, m$. Further the operator A consists of the spatial discretized parts, where operator B consists of the reaction and mobile-immobile parts of the full equation (15) and (16). Both parts can be computed independently.

We propose the following parallel scheme :

We compute m steps in parallel, for $j = 1, \ldots, m$ we compute in a parallel way:

$$\frac{\partial C_j(t)}{\partial t} = AC_j(t) \; + Q_j(t) \text{ , with } \; C_j(t^n) = C_j^n \tag{49}$$

and have the summarizing step :

$$\frac{\partial C_{m+1}(t)}{\partial t} = BC_{m+1}(t) \text{ , with } \; C_{m+1}(t^n) = \sum_{j=1}^{m} C_j^{n+1} \tag{50}$$

It we apply linear finite volume methods, we obtain for the one-dimensional problems a convergence order of $O(\tau + h^2)$.

The proof could be found in (Tai 1992).

4 EXPERIMENTS FOR THE MULTIPLE PHASE MODEL

In the following subsections, we present our experiments based on the mobile, immobile and adsorbed gaseous phases.

We contribute ideas to obtain an optimal layer-deposition, which is based on the PE-CVD process, while different additional phases are considered, e.g. plasma and precursor media.

The main contributions are an optimal collection of point sources, line sources or moving sources to cover the deposition area, with respect to the remainder concentration in the immobile and adsorbed phases.

We simulate the deposition process with our boundary value solver algorithms and could deal with many different conditions, that might be impossible for physical experiments. Such simulation results may benefit the physical experiment and give new ideas to optimize such deposition problems of a complicate physical prosces.

The next experiments show the deposition rates for different sources and their optimal positions in the apparatus. We concentrate on different exchange rates for the immobile and adsorbed phases, such concentrations are lost in the deposition process and they are very important to simulate.

4.1 Experiments with adsorbed rate $\alpha = 4\ 10^{-14}$ and immobile rate $g = 8\ 10^{-14}$"

The exchange in the following experiments between the mobile and immobile concentrations is very low, it is about $g = 8\ 10^{-14}$,we assume less activities in the plasma environment. Further the exchange between the mobile and adsorbed mobile concentrations is also very low it is about $\alpha = 4\ 10^{-14}$, also the exchange rates between the immobile and adsorbed immobile concentration is the same as in the mobile and adsorbed mobile phases. In this part we will

make some experiments.

4.1.1 Point Sources

In the first experiment we will take just one point source with short time interval of time steps equal to 25, and with long time interval of time steps equal to 100. In a next experiment, we apply moving sources. Such different combination of sources allow to control the deposition area.

Here, we apply one point source at the position (50,20). The number of time steps is 25.

In Figure 4, we present the concentration of the one point source with short time interval.

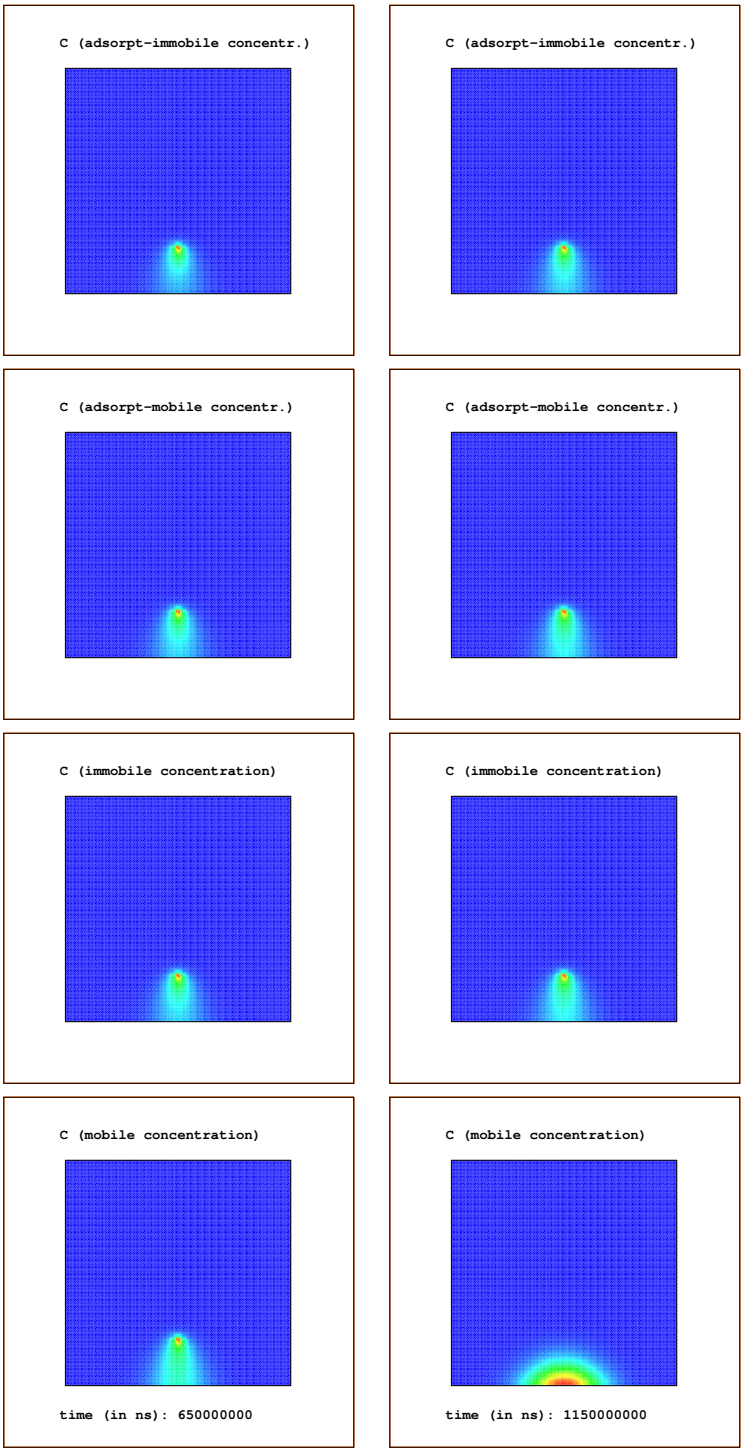

Figure 4: Simulation of one point source with immobile,mobile,adsorbed-mobile and adsorbed-immobile phases,the number of time-steps is 25.

In Figure 5, we present the deposition rates of the immobile concentration with point source,the number of time-steps is 25.

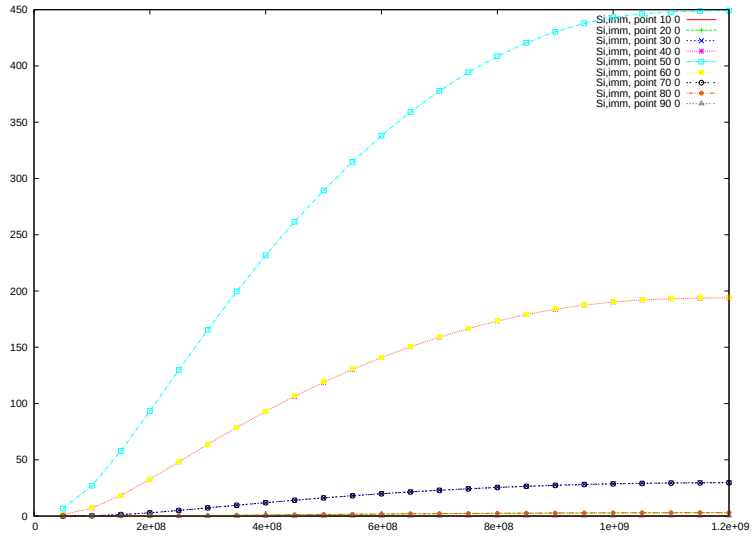

Figure 5: Deposition rates in case of immobile concentration and one point source,number of time-steps is 25.

In Figure 6, we present the deposition rates of the mobile concentration with one point source, we apply 25 time steps.

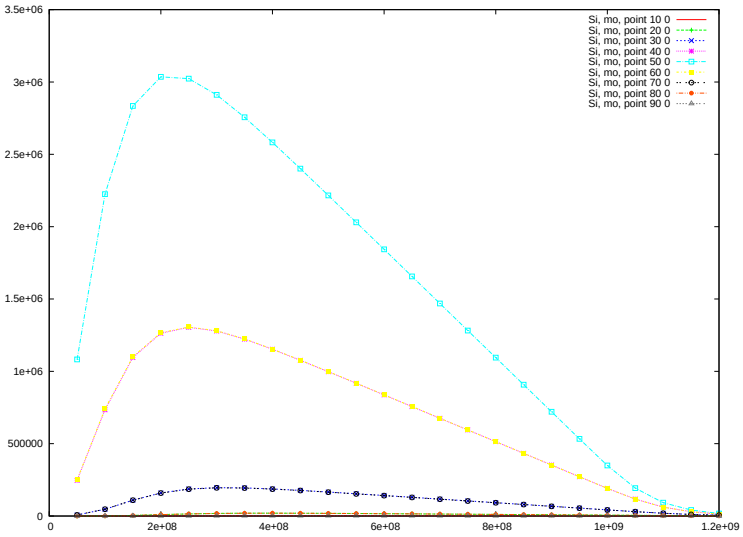

Figure 6: Deposition rates in case of mobile concentration and one point source, number of time-steps is 25.

In Figure 7, we show the deposition rates of the adsorpted-immobile concentration and one point source, we apply 25 time steps.

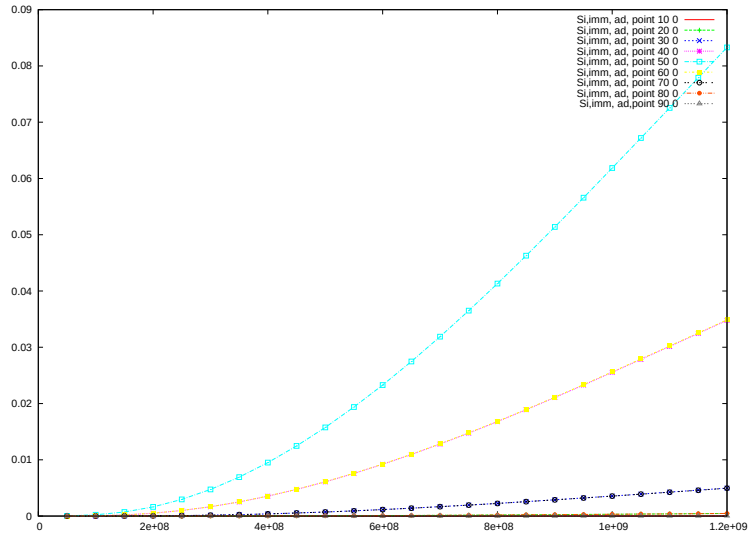

Figure 7: Deposition rates in case of adsorpted-immobile concentration and one point source, with number of time-steps equal to 25.

In Figure 8, we show the deposition rates of the adsorpted-mobile concentration and one point source, with number of time-steps equal to 25.

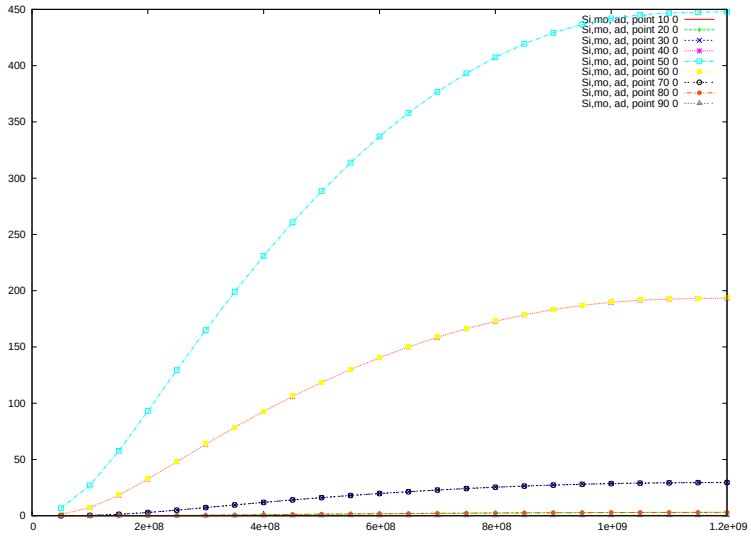

Figure 8: Deposition rates in case of adsorpted-mobile concentration and one point source, with number of time-steps equal to 25.

Remark 4 *We simulate in the first experiment the lost of concentration in the immobile and adsorpted phases with one point mobile source. Based on the low exchange rates for the immo-*

bile and adsorpted phases, we can see that the mobile concentration deposits without any lost of its concentration, the lost concentration is at least ander 0,000166 percent, and without any problems. next experiments have to be done to see that also multiple sources will not inflect the deposition rates. Also higher exchange rates have to be done to see such influences.

4.1.2 Moving Sources

In previus experiments see (Geiser and Arab 2008) we recieved best results in combining between point and line sources,and we use moving sources. In this experiment we will take 11 point sources at the positions Y =20,21,22,23,24,25,26,27,28,29,30 and these sources are moving in X direction in step equal to 15, the consintration hase value in each step equal to 1, X moves from $50 \rightarrow 35 \rightarrow 20 \rightarrow 35 \rightarrow 50 \rightarrow 65 \rightarrow 80 \rightarrow 65 \rightarrow 50$, we can switch these sources on and off. we gain moving soueces in X direction with $\Delta X = 15$. Concentrations in each step equal to 1 with short time.

In Figure 9, we present the experiment with 11 moving sources at the positions
Y =20,21,22,23,24,25,26,27,28,29,30 and these sources are moving in X direction in step equal to 15. The concentration is given value in each step with 1,X moves from $50 \rightarrow 35 \rightarrow 20 \rightarrow 35 \rightarrow 50 \rightarrow 65 \rightarrow 80 \rightarrow 65 \rightarrow 50$, with number of timestep equal to 25.

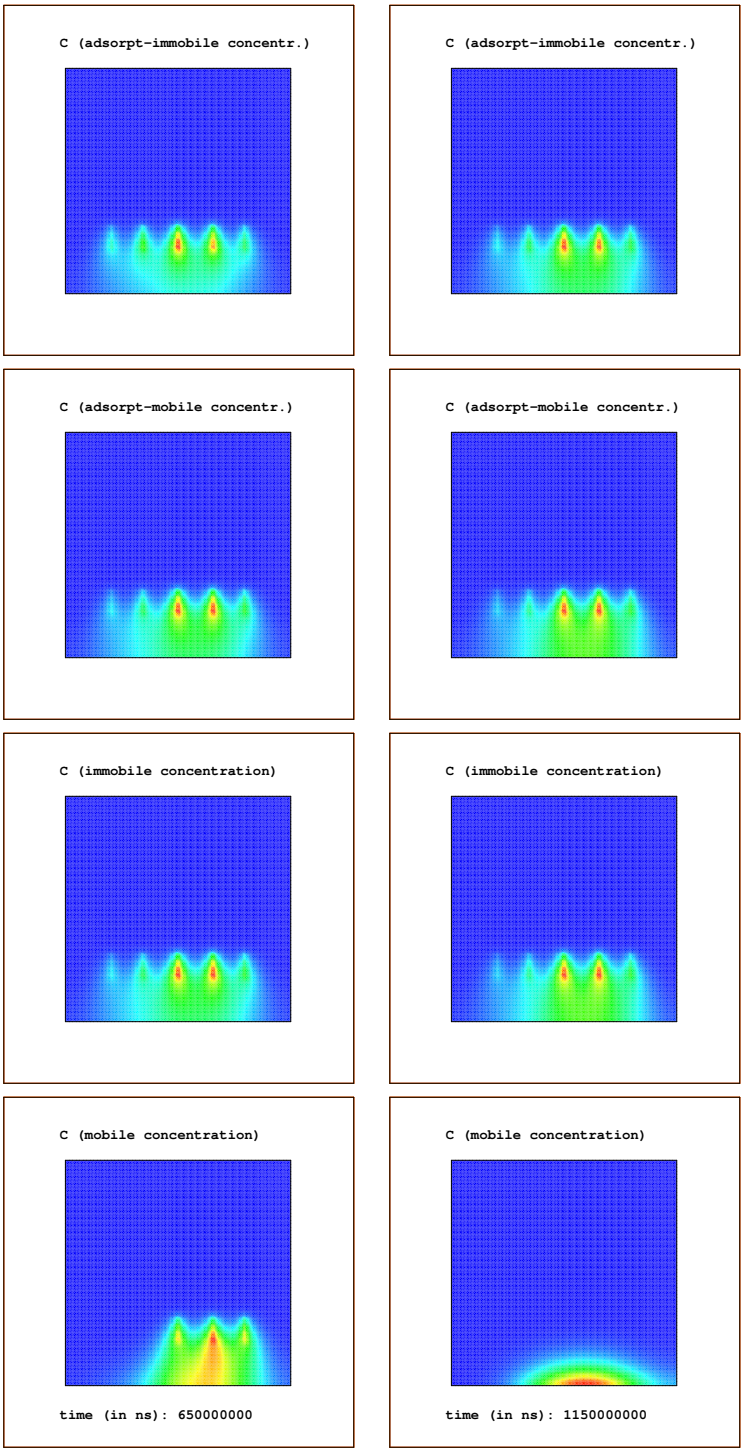

Figure 9: Immobile,mobile,adsorpted-mobile and adsorpted-immobile case of 11 moving sources moving in X direction in step equal to 15, X moves from $50 \rightarrow 35 \rightarrow 20 \rightarrow 35 \rightarrow 50 \rightarrow 65 \rightarrow 80 \rightarrow 65 \rightarrow 50$, with number of timestep equal to 25.

In Figure 10, we present the deposition rate of immobile concentration of 11 moving sources

moving in X direction in step equal to 15,X moves from $50 \rightarrow 35 \rightarrow 20 \rightarrow 35 \rightarrow 50 \rightarrow 65 \rightarrow 80 \rightarrow 65 \rightarrow 50$,with number of time steps equal to 25.

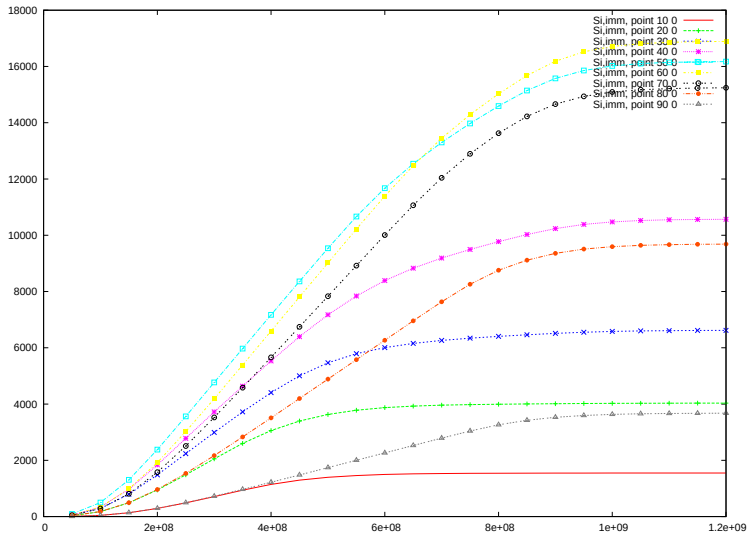

Figure 10: Deposition rates in case of immobile concentration of 11 moving sources moving in X direction in step equal to 15,X moves from $50 \rightarrow 35 \rightarrow 20 \rightarrow 35 \rightarrow 50 \rightarrow 65 \rightarrow 80 \rightarrow 65 \rightarrow 50$,with number of time step equal to 25.

In Figure 11, we present the deposition rate of mobile concentartion of 11 moving sources moving in X direction in step equal to 15,X moves from $50 \rightarrow 35 \rightarrow 20 \rightarrow 35 \rightarrow 50 \rightarrow 65 \rightarrow 80 \rightarrow 65 \rightarrow 50$,with number of time steps equal to 25.

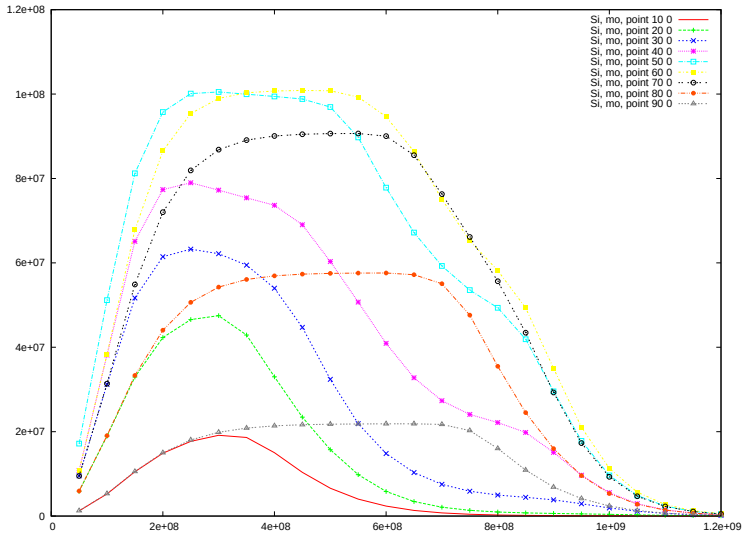

Figure 11: Deposition rates in case of mobile concentration of 11 moving sources moving in X direction in step equal to 15,X moves from $50 \rightarrow 35 \rightarrow 20 \rightarrow 35 \rightarrow 50 \rightarrow 65 \rightarrow 80 \rightarrow 65 \rightarrow 50$, with number of time steps equal to 25.

In Figure 12, we present the deposition rate of adsorpted-immobile concentration of 11 moving sources moving in X direction in step equal to 15,X moves from $50 \rightarrow 35 \rightarrow 20 \rightarrow 35 \rightarrow 50 \rightarrow 65 \rightarrow 80 \rightarrow 65 \rightarrow 50$,with number of time steps equal to 25.

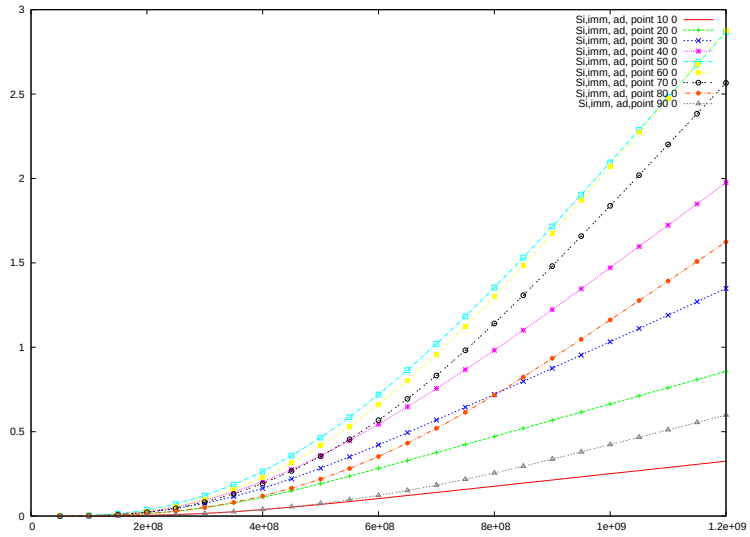

Figure 12: Deposition rates in case of adsorpted-immobile concentration of 11 moving sources moving in X direction in step equal to 15,X moves from $50 \rightarrow 35 \rightarrow 20 \rightarrow 35 \rightarrow 50 \rightarrow 65 \rightarrow 80 \rightarrow 65 \rightarrow 50$,with number of time step equal to 25.

In Figure 13, we present the deposition rate of adsorpted-mobile concentartion of 11 moving sources moving in X direction in step equal to 15,X moves from $50 \rightarrow 35 \rightarrow 20 \rightarrow 35 \rightarrow 50 \rightarrow 65 \rightarrow 80 \rightarrow 65 \rightarrow 50$,with number of time steps equal to 25.

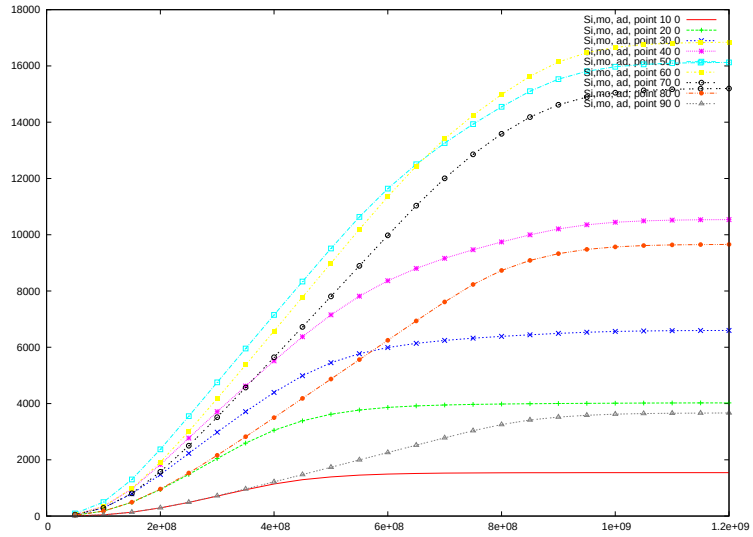

Figure 13: Deposition rates in case of adsorpted-mobile concentration of 11 moving sources moving in X direction in step equal to 15, X moves from $50 \rightarrow 35 \rightarrow 20 \rightarrow 35 \rightarrow 50 \rightarrow 65 \rightarrow 80 \rightarrow 65 \rightarrow 50$, with number of time steps equal to 25.

Remark 5 *With moving sources we gain improved deposition rates, also thediscussion in see (Geiser and Arab 2008). Nevertheless the remaining concentration in the immobile and adsorpted phases are important. In figure 13 and 10 we have at least a maximum of 18000[mol]; in each phase, but in percentage we lost only 0.00018 percent concentration. Du to this fact the higher deposition rates have at least the same percentage of lost concentration. Here moving sources have also the benefit of homogenized deposition rates.*

4.2 Experiments with adsorbed rate $\alpha = 4\ 10^{-14}$, immobile rate $g = 8\ 10^{-14}$

We change to deal with high exchange rates between the mobile and immobile gas concentration. Here we assume a high active plasma environment that influence the gaseous flow and retarded the concentration in the mobile phase. Such an influence can effect the deposition process . In this next experiments, we simulate the high reactive plasma influence with point sources.

We apply one point at (50,20) source with long time behaviour over 100 time steps. Such experiments can verify the optimum deposition area with different exchange rates.

In Figure 14, we present the concentration of the one point source with long time behaviour for all four phases, at different time points.

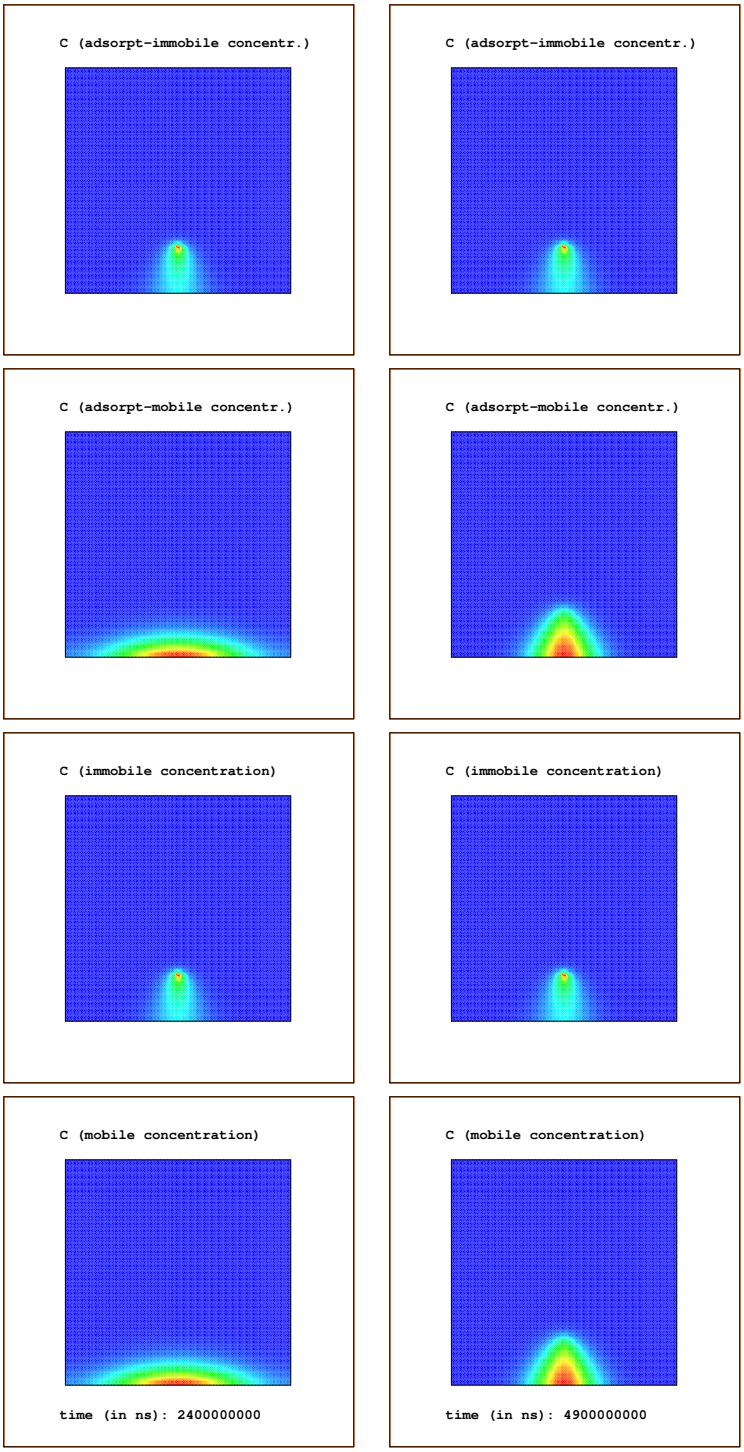

Figure 14: One point source,with immobile, mobile, immobile adsorpted and mobile adsorpted phases,the number of time-steps is 100.

In Figure 15, we show the deposition rates of the immobile concentration with one point source, number of time-steps is 100.

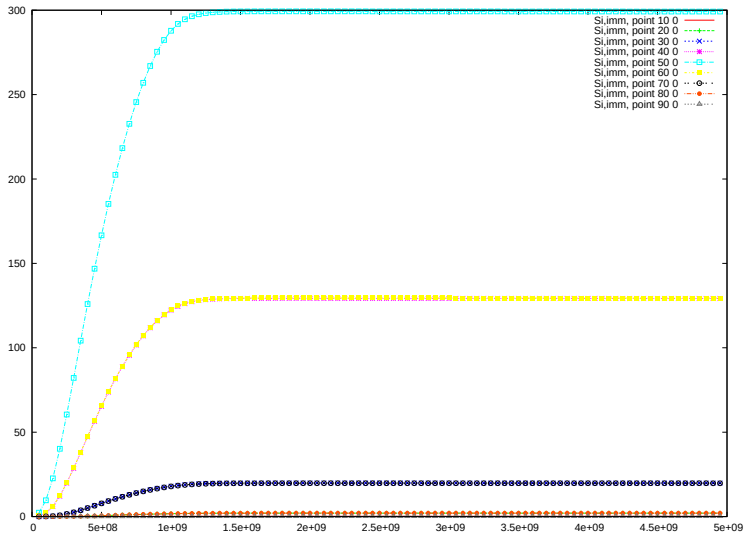

Figure 15: Deposition rates in case of immobile concentration and one point source, with number of time-steps equal to 100.

In Figure 16, we show the deposition rates of the mobile concentration and one point source, with number of time-steps equal to 100.

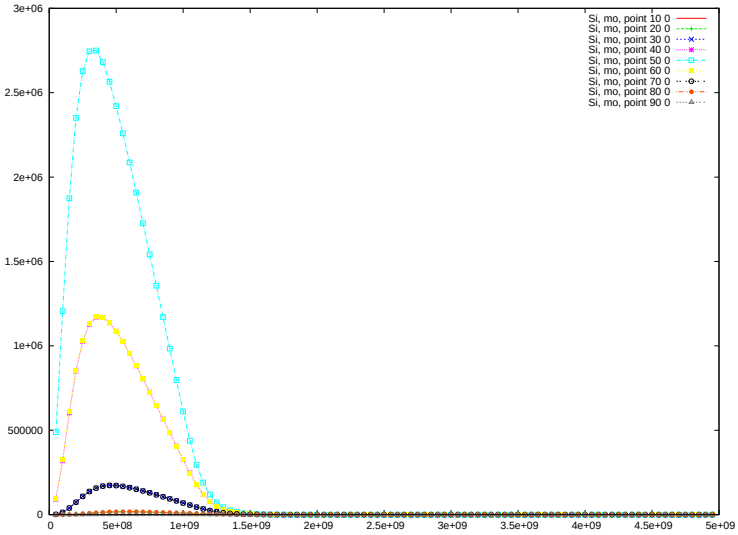

Figure 16: Deposition rates in case of mobile concentration and one point source, with number of time-steps equal to 100.

In Figure 17, we show the deposition rates of the adsorpted-immobile concentration and one point source, with number of time-steps equal to 100.

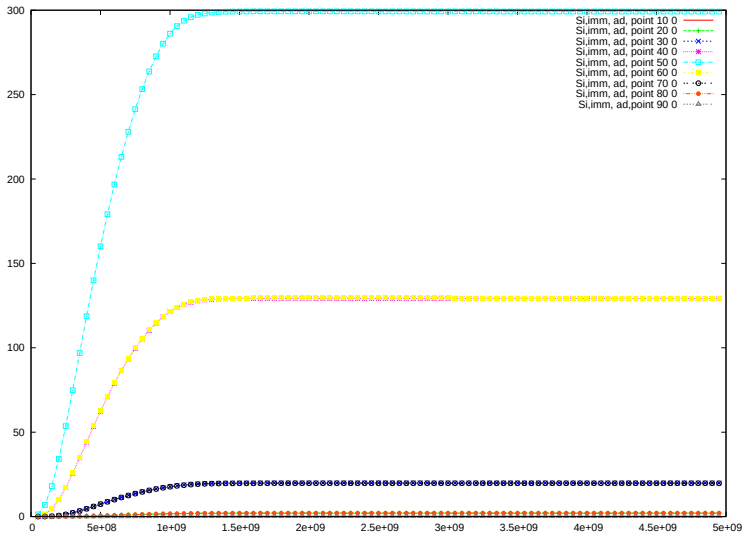

Figure 17: Deposition rates in case of adsorpted-immobile concentration and one point source, with number of time-steps equal to 100.

In Figure 18, we show the deposition rates of the adsorpted-mobile concentration and one point source, with number of time-steps equal to 100.

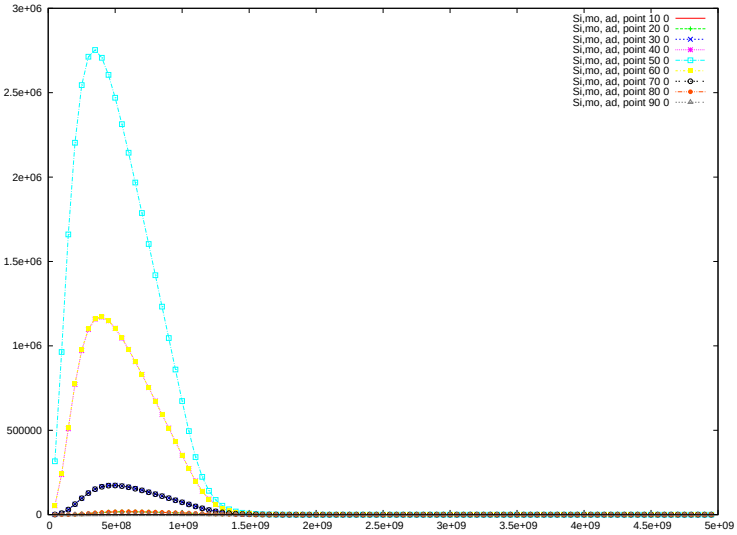

Figure 18: Deposition rates in case of adsorpted-mobile concentration and one point source, with number of time-steps equal to 100.

Remark 6 *The deposition rates reflect the high exchange rates of the mobile adsorpted phase. By the way the very lost exchange rates did not influence the deposition rates of the mobile concentration. Because of the fast exchange, the retardation in the adsorpted-mobile phase is not strong enough to prohibit to readsorpt to the mobile phase. At least high exchange rate do not influence the deposition processes.*

Remark 7 *We additionaly also did experiments with low exchange rates of adsorpted and mobile concentration and high exchange rates of mobile and immobile concentration. At least the results are equal to our results.*

4.3 Experiments with adsorbed rate $\alpha = 4\ 10^{-8}$, immobile rate $g = 8\ 10^{-8}$

The next experimnts deal with high exchange rates between the mobile and immobile gas concentration ,and also high exchange rates between the adsorpted and mobile/immobile gas concentration.

Here we assume a high reactive plasma environment and also a high reactive process gasenvironment, both processes can influence the flow of the mobile gas phases. To understand delecate process we simulate with various sources and measser the deopsition rates of the layer surface.

Here we concentrate on moving sources, because of their benefits to the homogeneous deposition rates, see (Geiser and Arab 2008).

To understand the exchange behaviour in the phases, we apply our best deposition experiment with moving sources.In this part we do one experimnt ,and apply 11 moving sources at the positions Y =20,21,22,23,24,25,26,27,28,29,30 and these sources are moving in X direction in steps equal to 15, the concentration isequal in each step to 1, X moves from $50 \rightarrow 35 \rightarrow 20 \rightarrow 35 \rightarrow 50 \rightarrow 65 \rightarrow 80 \rightarrow 65 \rightarrow 50$, with long time (The number of time steps is 100).

In Figure 19, we present an experiment with 11 moving sources at the positions
Y =20,21,22,23,24,25,26,27,28,29,30 and these sources are moving in X direction in step equal to 15. The concentration is equal to 1 in each step, X moves from $50 \rightarrow 35 \rightarrow 20 \rightarrow 35 \rightarrow 50 \rightarrow 65 \rightarrow 80 \rightarrow 65 \rightarrow 50$, with number of timestep equal to 100.

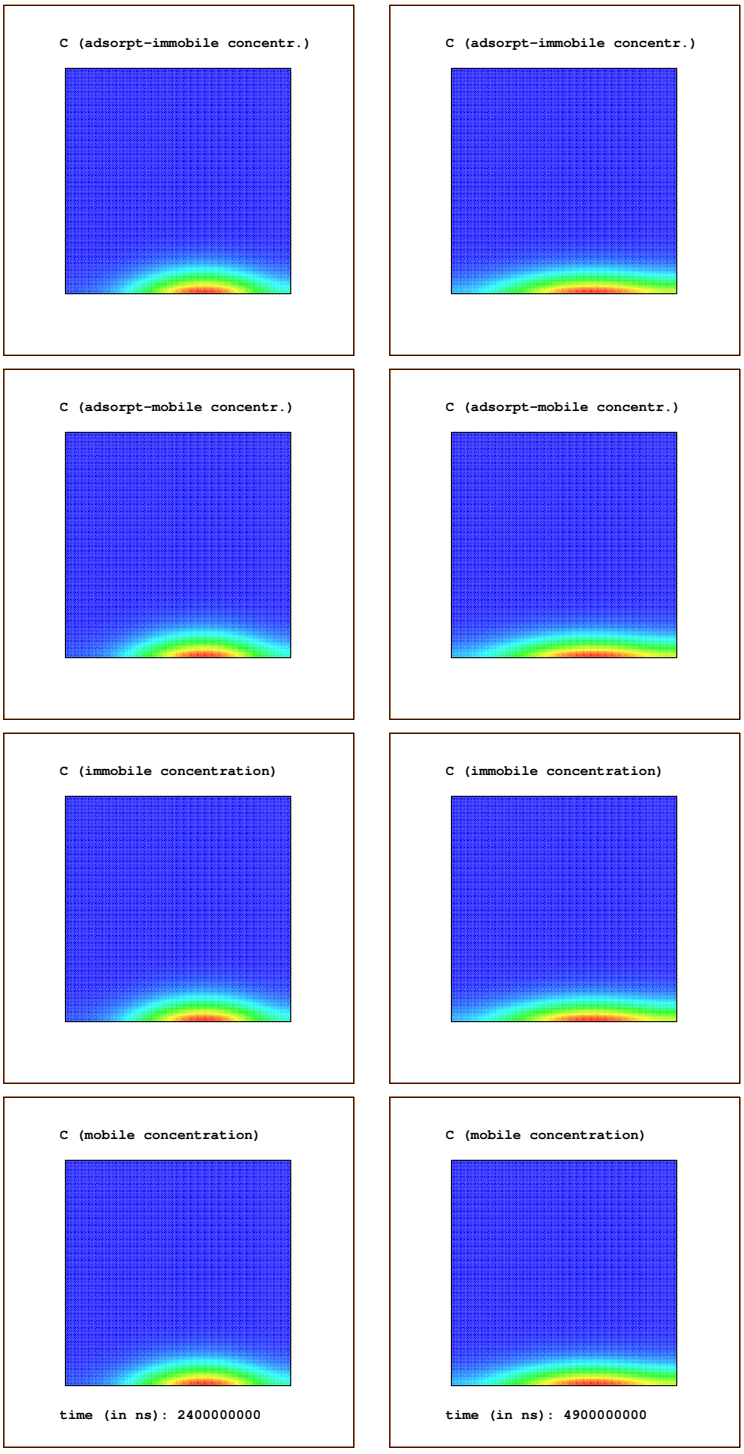

Figure 19: Immobile,mobile,adsorpted-mobile and adsorpted-immobile case of 11 moving sources moving in X direction in step equal to 15, X moves from $50 \rightarrow 35 \rightarrow 20 \rightarrow 35 \rightarrow 50 \rightarrow 65 \rightarrow 80 \rightarrow 65 \rightarrow 50$, with number of timestep equal to 100.

In Figure 20, we present the deposition rate of immobile concenration of 11 moving sources

moving in X direction in step equal to 15,X moves from $50 \rightarrow 35 \rightarrow 20 \rightarrow 35 \rightarrow 50 \rightarrow 65 \rightarrow 80 \rightarrow 65 \rightarrow 50$,with number of timestep equal to 100.

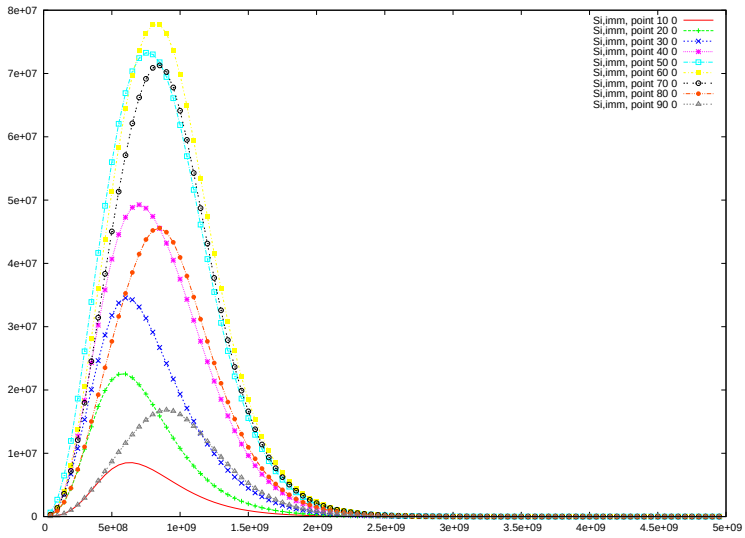

Figure 20: Deposition rates in case of immobile concentration of 11 moving sources moving in X direction in step equal to 15,X moves from $50 \rightarrow 35 \rightarrow 20 \rightarrow 35 \rightarrow 50 \rightarrow 65 \rightarrow 80 \rightarrow 65 \rightarrow 50$,with number of timestep equal to 100.

In Figure 21, we present the deposition rate of mobile concentration of 11 moving sources moving in X direction in step equal to 15,X moves from $50 \rightarrow 35 \rightarrow 20 \rightarrow 35 \rightarrow 50 \rightarrow 65 \rightarrow 80 \rightarrow 65 \rightarrow 50$,with number of timestep equal to 100.

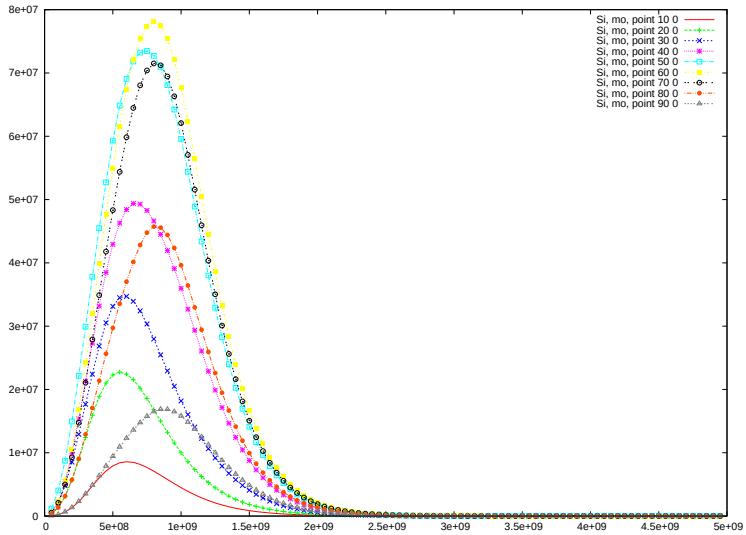

Figure 21: Deposition rates in case of mobile concentration of 11 moving sources moving in X direction in step equal to 15, X moves from $50 \rightarrow 35 \rightarrow 20 \rightarrow 35 \rightarrow 50 \rightarrow 65 \rightarrow 80 \rightarrow 65 \rightarrow 50$,with number of timestep equal to 100.

.

In Figure 22, we present the deposition rate of adsorpted-immobile concenration of 11 moving sources moving in X direction in step equal to 15,X moves from $50 \rightarrow 35 \rightarrow 20 \rightarrow 35 \rightarrow 50 \rightarrow 65 \rightarrow 80 \rightarrow 65 \rightarrow 50$,with number of timestep equal to 100.

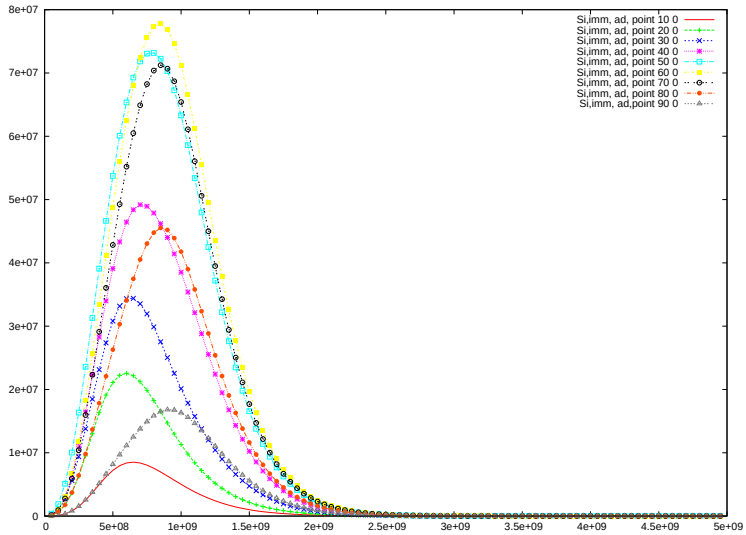

Figure 22: Deposition rates in case of adsorpted-immobile concentration of 11 moving sources moving in X direction in step equal to 15,X moves from $50 \rightarrow 35 \rightarrow 20 \rightarrow 35 \rightarrow 50 \rightarrow 65 \rightarrow 80 \rightarrow 65 \rightarrow 50$, with number of timestep equal to 100.

In Figure 23, we present the deposition rate of adsorpted-mobile concentration of 11 moving sources moving in X direction in step equal to 15,X moves from $50 \rightarrow 35 \rightarrow 20 \rightarrow 35 \rightarrow 50 \rightarrow 65 \rightarrow 80 \rightarrow 65 \rightarrow 50$,with number of timestep equal to 100.

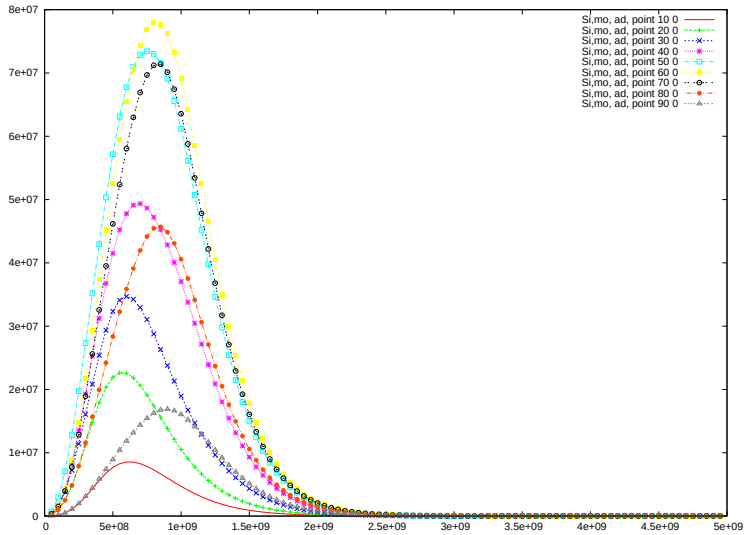

Figure 23: Deposition rates in case of adsorpted-mobile concentration of 11 moving sources moving in X direction in step equal to 15, X moves from $50 \rightarrow 35 \rightarrow 20 \rightarrow 35 \rightarrow 50 \rightarrow 65 \rightarrow 80 \rightarrow 65 \rightarrow 50$,with number of timestep equal to 100.

.

Remark 8 *Respecting high exchange rates for all phases , means an influence to the gaseous flow of our deposition gas.Nevertheless the lost exchange process measures arereversible, that means that adsorpted and immobile gas concentartion can readsorpted to the mobile phase as we see in figures 20 - 23, that all concentration are nearly equal, that means the influence to the mobile phase is not so important. We obtain at least the same deposition rates as for the nun influenced gaseus flow. By the way minimal lost of concentration can be asuumed but this will not influence the deposition processes.*

5 CONCLUSIONS AND DISCUSSIONS

We have presented a continuous model for the multiple phases, we assumed gaseous behaviour with exchange rates to adsorpted and immobile phases at very low pressere and low temperature while dealing with catalyst processes, e.g. plasma environment and precursor gases. We have to taken into acount the remaining gas concentrations in each processes.Numerical experiments

presented the less influence of such catalyst processes, while fast processes did not acure in the time scales, and slow processes did not prohibit an important amount of the gas concentration. In future we are interested on analysing such fast processes due the very small time scales, e.g in a micro modell (Molecular dynamics model).

REFERENCES

Barsoum MW and El-Raghy T (1996). Synthesis and characterization of a remarkable ceramic: ti_3sic_2. *J.Am.Ceram.Soc. 79*(1), pp. 1953–1956.

Bear J (1972). *Dynamics of fluids in porous media*. American Elsevier, New York.

Cao, GZ Brinkman H Meijerink J DeVries KJ and Burggraaf AJ (1993). Kinetic study of the modified chemical vapour deposition process in porous media. *J.Mater.Chem. 3*(12), pp. 1307–1311.

Chapman B (1980). *Glow Discharge Processes. Sputering and Plasma Etching*. John Wiley & Sons, Inc. First Edition.

Dobkin MK and Zuraw DM (2003). *Principles of Chemical Vapor Deposition.* Springer, New York. First Edition.

Du, Y Schuster JC Seifert HJ and Aldinger F (2000). Experimental investigation and thermodynamic calculation of the titanium-silicon-carbon system. *J.Am.Ceram.Soc. 83*(1), pp. 193–203.

Farago I Geiser J (2005). Iterative operator-splitting methods for linear problems. Technical Report 1043, Weierstrass Institute for Applied Analysis and Stochastics, Berlin, Germany, Mohrenstrasse, Berlin, Germany.

Farooq S and Ruthven DM (1991). Dynamics of kinetically controlled binary adsorption in a fixed bed. *AIChE Journal. 37*(2), pp. 299–301.

Favia, P Sardella E Gristina R Millella A and D'Agostino R (2002). Functionalization of biomedical polymers by means of plasma processes: Plasma treated polymers with limited

hydrophobic recovery and pe-cvd of cooh functional coatings. *Journal of Polymer Science and Technology 15*(2), pp. 341–350.

Fein E (2004). Software package r^3t. Technical report.

Frolkovič P (2002a). Flux-based method of characteristics for contaminant transport in flowing groundwater. *Computing and Visualization in Science*.

Frolkovič P (2002b). Flux-based methods of characteristics for transport problems in groundwater flows induced by sources and sinks. *Computational Methods in Water Resources (S.M. Hassanizadeh et al.)Volume II., Elsevier, Amsterdam, Boston, Heidelberg,*.

Frolkovič P and De Schepper H (2001). Numerical modelling of convection dominated transport coupled with density driven flow in porous media. *Advances in Water Resources 24*.

Frolkovič P and Geiser J (2003). Discretization methods with discrete minimum and maximum property for convection dominated transport in porous media.

Geiser J (2003). *Gekoppelte Diskretisierungsverfahren für Systeme von Konvektions-Dispersions-Diffusions-Reaktionsgleichungen.* Ph. D. thesis, Universität Heidelberg.

Geiser J (2006). Discretisation methods with analytical solutions for convection-diffusion-dispersion-reaction-equations and applications. *Journal of Engineering Mathematics. 57*(1), pp. 79–98.

Geiser J and Arab M (2008). Modelling, optimzation and simulation for a chemical vapor deposition. *Journal of Porous Media*.

Glowinski R (2003). *Numerical methods for fluids.* Handbook of Numerical Analysis, Gen. eds. P.G. Ciarlet, J. Lions, Vol. IX, North-Holland Elsevier, Amsterdam, The Netherlands.

Gobbert MK and Ringhofer CA (1998). An asymptotic analysis for a model of chemical vapor deposition on a microstructured surface. *SIAM Journal on Applied Mathematics. 58*.

Higashi K and Pigford ThH (1980). Analytical models for migration of radionuclides in geologic sorbing media. *Journal of Nuclear Science and Technology 17(9)*.

Hlavacek, V Thiart J and Orlicki D (1995). Morphology and film growth in cvd reactions. *J. Phys. IV France 5*.

Jin S and Wang X (2002). Robust numerical simulation of porosity evolution in chemical vapor infiltration. *Journal of Computational Physics 179*(2), pp. 557–577.

Johannsen K (1999). *Robuste Mehrgitterverfahren für die Konvektions-Diffusions Gleichung mit wirbelbehafteter Konvektion*. Ph. D. thesis, University of Heidelberg, Germany.

Jury WA and Roth K (1990). *Transfer Functions and Solute Movement through Soil*. Basel, Boston, Berlin: Bikhäuser Verlag.

Lange, C Barsoum MW and Schaaf P (2007). Towards the synthesis of max-phase functional coatings by pulsed laser deposition. *Applied Surface Science 254*.

Lemieux, JM Chambreau SD and Zhang J (2008). Mixed silicon-germanium clusters, $si_xge_yh_z$, in the gas phase by flash pyrolysis of silane and germane. *Chemical Physics Letters. 459*.

Leveque RJ (2002). *Finite Volume Methods for Hyperbolic Problems.* Cambridge Texts in Applied Mathematics, Cambridge, UK.

Lieberman MA and Lichtenberg AJ (2005). *Principle of Plasma Discharges and Materials Processing.* Wiley-Interscience, AA John Wiley & Sons, Inc Publication. second Edition.

Morosoff N (1990). *Plasma Deposition, Treatment and Etching of Polymers*. R. d'Agostino ed., Acad. Press. First Edition.

Ohring M (2002). *Materials Science of Thin Films.* Academic Press, San Diego, New York, Boston, London. Second Edition.

Rouch H (2006). Mocvd research reactor simulation. *Proceedings of the COMSOL Users Conference 2006 Paris*, Paris, France.

Scheidegger AE (1961). General theory of dispersion in porous media. *Journal of Geophysical Research 66*.

Senega TK and Brinkmann RP (2007). Generalized transport coefficients of multicomponent low-temperature plasmas.

Serdyuk YV and Gubanski SM (2005). Computer modeling of interaction of gas discharge plasma with solid dielectric barriers. *Dielectrics and Electrical Insulation, IEEE Transactions on 12*(4), pp. 725–735.

Tai XC (1992). Global extrapolation with parallel splitting method. *Numerical Algorithms 3*.